Phase behavior of polyelectrolyte solutions with salt

Chi-Lun Lee and Murugappan Muthukumar

Citation: The Journal of Chemical Physics **130**, 024904 (2009); doi: 10.1063/1.3054140
View online: http://dx.doi.org/10.1063/1.3054140
View Table of Contents: http://scitation.aip.org/content/aip/journal/jcp/130/2?ver=pdfcov
Published by the AIP Publishing

Phase behavior of polyelectrolyte solutions with salt

Chi-Lun Lee[a] and Murugappan Muthukumar[b]
Department of Polymer Science and Engineering, University of Massachusetts, Amherst, Massachusetts 01003, USA

(Received 28 July 2008; accepted 26 November 2008; published online 14 January 2009)

We have computed the phase diagrams of solutions of flexible polyelectrolyte chains with added simple electrolytes. The calculations are based on our recent theory [M. Muthukumar, Macromolecules **35**, 9142 (2002)], which accounts for conformational fluctuations of chains, charge density correlations arising from dissolved ions, hydrophobic interaction between polymer backbone and solvent, and translational entropy of all species in the system. The theory is at the mean field level and recovers the results of the restricted primitive model with the Debye–Hückel description for solutions of simple electrolytes without any polymer chains and those of the Flory–Huggins and scaling theories for uncharged polymers in the absence of charges or electrolytes. In constructing the phase diagrams, the chemical potential of each of the species is maintained to be the same in the coexisting phases and at the same time each phase being electrically neutral (Donnan equilibrium). Comparisons are made with a more constrained situation where the chemical potentials of the independent components are maintained to be the same in the coexisting phases. Our calculations predict several rich phenomena. Even for the salt-free solutions, two critical phenomena (corresponding to the Flory–Huggins-type and the restricted-primitive-model-type critical points) are predicted. The coupling between these two leads to two critical end points and triple points. In the presence of salt, the valency of electrolyte ions is found to influence drastically the phase diagrams. Specifically, the predicted liquid-liquid phase transitions in certain temperature ranges is reminiscent of the re-entrant-precipitation phenomenon observed experimentally for polyelectrolytes condensed with trivalent salts. © *2009 American Institute of Physics*.
[DOI: 10.1063/1.3054140]

I. INTRODUCTION

The phase behavior of polyelectrolyte solutions has been one of the challenging problems in polymer science and technology.[1–11] The challenge for a reliable theoretical formulation[12–28] is compounded by the long range correlations arising from electrostatic interactions and the topological connectivity of the polymer chains. Furthermore, the system consists of multiple length scales, such as the monomer size, counterion radius, radii of dissociated salt ions, molecular size of solvent, radius of gyration of the polymer, and correlation lengths for the electrostatics and polymer concentration fluctuations.

On the experimental side, while there are many reports[1–11] on polyelectrolyte phase behavior, systematic investigations are only at initial stages. This is largely due to the vastness of the parameter space for systematic experimental study. The results depend drastically on many variables such as length, charge density, backbone stiffness and sequence of charged groups of the polyelectrolyte, identity (sign, size, and valency) of counterions and dissociated salt ions, and dielectric inhomogeneity of the solution. Typically, studies have been carried out at room temperatures to find out whether mixtures of fixed compositions of polyelectrolytes and other additives (such as other polyelectrolytes and nonionic polymers, surfactants) are soluble at this temperature. Notable examples[1–4] are the precipitation studies of solutions of polyelectrolytes such as sodium-poly(styrene sulfonate) and single stranded-DNA by trivalent salts such as lanthanum trichloride. A universal reentrant phenomenon has been observed in these precipitation studies at room temperatures. For a given polyelectrolyte concentration, precipitation is observed as the salt concentration C_s is increased. If C_s is increased further, the precipitate becomes soluble again. The range of C_s for the precipitation of the polymer decreases as the polyelectrolyte concentration is increased. One of the goals of the present theory is to shed light on this re-entrant phenomenon.

The effect of temperature on the polyelectrolyte phase behavior has been previously carried out in our laboratory.[9–11] The system is the ternary solution of sodium-poly(styrene sulfonate), barium chloride, and water. At room temperatures, an increase in salt concentration leads to precipitation and the threshold C_s for precipitation increases with the polymer concentration C_p. For this particular system, no resolubilization at higher C_s is observed. By varying the temperature and using a combination of light, x-ray, and neutron scattering methods and microscopy, we have shown that the precipitation is the liquid-liquid coexistence phenomenon and that the critical behavior near the coexistence curve is reminiscent of the three-dimensional Ising univer-

[a]Present address: Department of Physics, National Central University, Jhongli 32001, Taiwan.
[b]Author to whom correspondence should be addressed. Electronic addresses: muthu@polysci.umass.edu and jcpeditor@chem.ucsb.edu.

sality class. Analogously, the re-entrant precipitation by trivalent ions might be related to liquid-liquid coexistence.

At the outset, two extreme situations of polymer solutions may be imagined. In one extreme, we deal with uncharged polymer solutions, and the Flory–Huggins (FH) theory[29] developed in the premise of mean-field approximations has been found to be very successful in explaining many experimental phenomena dealing with phase behavior of polymer solutions and blends. In the other extreme of electrolyte solutions without any polymerized chains, the Debye–Hückel theory[30] for the restricted primitive model[31,32] (DH+RPM) has been found to be an excellent mean-field description.[33,34] It would be desirable to compose a general mean-field theory for polyelectrolyte solutions that reduces to these extreme limits of FH and DH+RPM. Such theory was recently derived[27] by one of the authors (M), which bridges the Flory–Huggins theory of polymer solutions and the DH+RPM theory of simple electrolytes. Basically, this theory accounts for (a) the translational entropy of polymer chains, counterions, dissolved ions and solvent molecules, (b) two-body interactions among monomers mediated by solvent and dissociated ions, (c) electrostatic correlations arising from the extended Debye-Hückel treatment, and (d) conformational fluctuations of the polymer. Specific effects arising from solvation of ions and ion bridges are ignored.[35–38] In the present paper, we implement the M theory in deriving the phase behavior of polyelectrolyte solutions with added salt.

Prior to the development of the M theory, there have been several theoretical attempts. The theory by Mahdi and de la Cruz[14] to obtain free energy expressions using the random phase approximation (RPA) led to strange results. For example, for salt-free polyelectrolyte solutions, polyelectrolyte networks and solutions were to be coexisting if the degree of polymerization N is greater than a critical value $N^* \simeq 30$; for $N<N^*$, the usual liquid-liquid coexistence were to be present. Such strange predictions can be traced to the qualitative inadequacy of the RPA for polyelectrolyte solutions. According to the RPA, the correlation length for monomer density ξ scales with polymer concentration C_p as $\xi \sim C_p^{-1/4}$ in salt-free solutions, so that the free energy is proportional to $C_p^{3/4}$. Consequently the osmotic pressure Π from RPA term $(\Pi \sim 1/C_p^{1/4})$ diverges nonphysically as $C_p \to 0$, which was then cured by mathematically motivated cutoffs. A proper theoretical treatment should give $\xi \sim C_p^{-1/2}$ (for salt-free solutions) so that $\Pi \sim C_p^{1/2}$ without any divergence difficulties.

The dominant contribution from the counterion entropy was recognized by Khokhlov and Nyrkova,[24] who defined an effective molar mass, which is to be much smaller than the nominal molar mass. This led to the qualitative result of very significant compatibility enhancement. However, physical volume of counterions and their electrostatic correlations, and chain fluctuations were ignored. Same approach was taken by Warren,[20] who computed coexistence curves and spinodal curves. The consequences of including volume of counterions in the free energy expression were addressed by Gottschalk *et al.*,[22] who compared their "explicit counterions' approach against the "effective length" approximation of Khokhlov and Nyrkova. Again, the only contribution from the ions to the free energy is the entropy of mixing (in combination with the electroneutrality constraint), without any corrections from fluctuations in charge density of dissociated ions and in polymer density.

In the present paper, we report predictions of phase behavior for ternary solutions containing polyelectrolyte, simple salt, and solvent, based on the theory of Muthukumar.[27] In the original work, phase diagrams for the two-component salt-free solutions were presented. The current extension to the presence of added salt requires minimization of the Helmholtz free energy in a multidimensional space. When the polyelectrolyte solution undergoes thermodynamic instability, the chemical potential of each of the components in the system must be made equal in the coexisting phases. In the case of uncharged three-component systems, the construction of coexistence curves requires equality of three chemical potentials (corresponding to the three components) in the coexisting phases. This in turn requires a minimization procedure in a three-dimensional space. On the other hand, for polyelectrolyte solutions containing salt, chemical potentials of five species (polymer, counterions, cations and anions of added salt, and solvent) must be equated in the coexisting phases, while at the same time maintaining electroneutrality of each phase (Donnan equilibrium). This requires minimization of the Helmholtz free energy in a four-dimensional space, as explained in Sec. II. We have performed calculations in conformity with the Donnan criterion and compared with the restricted condition of equating chemical potentials of the three components (polyelectrolyte, salt, and solvent) in the coexisting phases.

It must be noted that both the chemical mismatch (Flory–Huggins) χ parameter and the Coulomb strength (Bjerrum length ℓ_B) depend on the temperature T. Therefore, when the temperature is altered in an experiment, both χ and ℓ_B change. In view of this, we have defined a reduced temperature t as a reciprocal of ℓ_B, and χ is written to be proportional to a/t, where a is taken as the hydrophobicity parameter. In our computed phase diagrams, when t is changed, both χ and ℓ_B change.

We find the emergence of two kinds of liquid-liquid phase separations, one corresponding to the hydrophobic effect (analogous to the FH type) and the other corresponding to the electrostatic effect (analogous to the RPM type). The interference between these two kinds leads to triple points for sufficiently large values of hydrophobicity and degree of ionization. Depending on the values of the parameters, the two critical phenomena of liquid-liquid phase separations lead to critical end points. The presence of multivalent ions is found to drastically affect the phase behavior. Indeed, the calculated liquid-liquid coexistence curve for the three component solutions with trivalent cations resemble remarkably the "precipitation curve" observed experimentally.

The rest of the paper is organized as follows. Section II gives a quick list of the various terms used in the free energy, without repeating the original theory in Ref. 27, and a description of the computational methods. The results and their discussion are presented in Sec. III, followed by a concluding section.

II. MODEL

The present theory is an extension of our earlier work[27] to multicomponent polyelectrolyte solutions. The theoretical basis for the underlying assumptions behind the model is outlined in Refs. 26 and 27. Only a brief account of the starting point for the free energy expression is given below, and the original references need to be consulted for the derivation of the free energy of the system. The essential feature of our theory is its reducibility to the FH theory of polymer solutions, when the charges are absent, and to the DH+RPM of simple electrolytes, when the degree of polymerization of the polyelectrolyte is taken to be unity. The present theory offers a crossover description between these two classical limits of FH and DH+RPM in terms of degree of ionization of the polyelectrolyte, the strength and range of Coulomb interaction, and the strength of the hydrophobic interaction between the polymer backbone and the solvent. The role of fluctuations of polymer conformations and spatial distribution of counterions and electrolyte ions is also included.

We consider a solution of n polyelectrolyte chains, each with N Kuhn segments, dispersed in a solvent with n_0 uncharged solvent molecules. Due to the ionic equilibria of the ionizable repeat units of the chain and the counterion adsorption[37] on the chain, let α be the effective degree of ionization and Z_p be the effective valency of each segment so that each segment has an effective charge of $Z_p\alpha$. To maintain the electroneutrality of the solution, the total number of unadsorbed counterions in the solution is $\alpha Z_p nN/Z_c$, with Z_c being the valency of the counterion. In addition, let n_+ and n_- ions, with Z_+ and Z_- valencies, respectively, be present in the solution from the added salt. Again, due to the charge neutrality of the whole solution, $n_-=n_+Z_+/Z_-$. For simplicity of the calculations, without loss of generality, we assume that all ions, polymer segments and solvent molecules are all spherical with the identical volume $\pi\ell^3/6$, and polymer chains are modeled as the freely jointed chain of hard spheres. The interactions in the system include volume exclusion, short-ranged pairwise interaction among neutral molecules and neutral groups of polymer segments, and the long-ranged Coulomb interactions among dissociated ions and ionized polymer segments. The dielectric constant ϵ is assumed to be uniform in the solution. We assume the solution to be incompressible with a total volume Ω.

The statistical mechanics of polyelectrolyte solutions with added salt is rather complicated. The difficulty is attributed to both the polymer connectivity and the long-ranged Coulomb interactions between charged particles. As derived in Ref. 26 the partition function of a modeled polyelectrolyte solution can be treated in a way such that the "fast" modes, namely, the degrees of freedom for small ions, are integrated first via a RPA, viewing that small ions have a fast relaxation time and will form a shielding cloud according to the polymer configuration. This approximation leads to an effective pair interaction among ionized polymer segments, with the Debye–Hückel form. The Debye screening length κ^{-1} depends on the concentrations of the unadsorbed counterions and the added salt ions and not directly on the polymer concentration. The corresponding free energy expression is analogous to the Debye–Hückel free energy, capturing the fluctuations of the small ions. When polymers interpenetrate above the overlap concentration, the intramolecular electrostatic screening between pairs of segments is further screened, labeled as the double screening.[26] The integration over all allowed polymer conformations gives the Helmholtz free energy F of the system. The final result for the Helmholtz free energy can be written as

$$\frac{\ell^3 F}{\Omega k_B T} = f_S + f_H + f_{\mathrm{fl},i} + f_{\mathrm{fl},p}, \tag{2.1}$$

where k_BT is the Boltzmann constant times the absolute temperature, and f_S represents the mixing entropy of ions, solvent molecules, and polymer chains. The second term f_H represents the mean-field mixing enthalpy for polymer chains and solvent, while the third term $f_{\mathrm{fl},i}$ arises from fluctuations in the distribution of dissociated ions. The fourth term in Eq. (2.1), $f_{\mathrm{fl},p}$, is related to fluctuations in the distribution and conformations of polymers. Following Ref. 27 the entropy part f_S in Eq. (2.1) is given by

$$f_S = \frac{\Phi}{N}\ln\Phi + \Phi_c \ln\Phi_c + \Phi_0 \ln\Phi_0 + \Phi_+ \ln\Phi_+ + \Phi_- \ln\Phi_- \tag{2.2}$$

where $\Phi=nN\ell^3/\Omega$ is the volume fraction of polymers, $\Phi_c=\alpha_1\Phi$ is the volume fraction of counterions from dissolved polyelectrolyte ($\alpha_1=\alpha Z_p/Z_c$ due to charge neutrality), $\Phi_+=n_+\ell^3/\Omega$ and $\Phi_-=n_-\ell^3/\Omega$ are volume fractions of salt cations and anions, respectively, and $\Phi_0=1-\Phi-\Phi_c-\Phi_+-\Phi_-$ is the volume fraction of solvent molecules.

The enthalpy part f_H in Eq. (2.1) is given by

$$f_H = \left(\frac{1}{2}w_{pp}\Phi^2 + \frac{1}{2}w_{ss}\Phi_0^2 + w_{ps}\Phi\Phi_0\right) + \Phi^2\left(\frac{2\pi\alpha^2 Z_p^2 \ell_B}{\kappa^2\ell^3}\right) \tag{2.3}$$

with

$$\kappa^2\ell^2 = 4\pi\frac{\ell_B}{\ell}[Z_c^2\Phi_c + Z_+^2\Phi_+ + Z_-^2\Phi_-], \tag{2.4}$$

where ℓ_B is the Bjerrum length

$$\ell_B = \frac{e^2}{4\pi\epsilon_0\epsilon k_B T}. \tag{2.5}$$

The enthalpy part of the free energy density represents the mean-field energy that includes the short-ranged interactions among solvent and neutral polyelectrolyte segments as well as the electrostatic interactions among polyelectrolyte segments. The short-ranged interactions can be represented via the Flory–Huggins parameter χ. The effective electrostatic energy between two charged polyelectrolyte segments has the Yukawa form $v(r)=Z_p^2\ell_B\exp(-\kappa r)/r$ with the inverse screening length κ defined by Eq. (2.4). The second term in Eq. (2.3) is valid when there are enough counterions and salt ions in the system. For polyelectrolyte concentrations relevant to investigations of phase behaviors of solutions, this approximation is adequate even for the "salt-free" solutions.

The free energy density due to ion fluctuations $f_{\mathrm{fl},i}$ is given by

$$f_{\mathrm{fl},i} = -\frac{1}{4\pi}\left[\ln(1+\kappa\ell) - \kappa\ell + \frac{1}{2}(\kappa\ell)^2\right]. \tag{2.6}$$

As in the Debye–Hückel theory, this is derived by solving a linearized Poisson–Boltzmann equation[27] for non-neutral charge plasma. Note that the Debye–Hückel limiting law (DHLL) is recovered in the limit $\ell \to 0$, $f_{\mathrm{fl},i} \to -(\kappa\ell)^3/(12\pi)$, as was derived in Ref. 26.

Finally, the free energy density due to polymer fluctuations $f_{\mathrm{fl},p}$, as derived in Ref. 26 for both cases of high-salt and low-salt limits, can be written down via a simple interpolation. It is given by

$$f_{\mathrm{fl},p} = \frac{\frac{2^{3/4}}{9}\sqrt{\frac{\pi}{3}}\left(\frac{3}{2}\right)^{-9/4}(4\pi Z_p^2\alpha^2\ell_B/\ell)^{3/4}\Phi^{9/4}}{(\kappa\ell)^{3/2} + 2^{5/4}\sqrt{\frac{\pi}{3}}\left(\frac{3}{2}\right)^{-3/4}(4\pi Z_p^2\alpha^2\ell_B/\ell)^{1/4}\Phi^{3/4}}. \tag{2.7}$$

In Eq. (2.7) one can find that $f_{\mathrm{fl},p} \sim \Phi^{3/2}$ in the low-salt limit and $f_{\mathrm{fl},p} \sim \Phi^{9/4}$ in the high-salt limit.[26] Throughout our calculations we find that the polymer fluctuations only play a minor role in deciding the location of phase boundary and, consequently, elaborate crossover descriptions for $f_{\mathrm{fl},p}$ provided in Ref. 26 are not addressed in the present work.

Because of charge neutrality ($\Phi_c Z_c = \alpha\Phi Z_p$ and $\Phi_- Z_- = \Phi_+ Z_+$) our modeled system of polyelectrolyte solution can be viewed as a ternary one with salt (both cations and anions), polyelectrolyte (including polymer chains and the corresponding dissolved cations), and solvent molecules. And their volume fractions are $C_s = \Phi_+ + \Phi_-$, $C_p = \Phi + \Phi_c$, Φ_0, respectively. Due to incompressibility, the total volume of the system Ω is fixed. For clarity, we represent all of our ternary phase diagrams as Cartesian C_s-C_p plots in the present paper. In a ternary diagram the boundary of phase separation is represented via binodal points. Each pair of binodal points is connected with a tie line. A point residing on a tie line will separate into two phases at its corresponding binodal points, and the amount of each phase is decided according to the lever rule.

In our numerical calculations we derive the binodal points via the minimization of the free energy.[39] For a phase separation in a ternary system, if a point (Φ_1, Φ_2, Φ_3) lies inside the phase boundary, it will demix into two phases with composition $(\Phi_1^A, \Phi_2^A, \Phi_3^A)$ in the A phase and composition $(\Phi_1^B, \Phi_2^B, \Phi_3^B)$ in the B phase. Let x be the fraction of the solution separating into the A phase and $1-x$ be the fraction separating into the B phase. Then one can write down the following relation (the lever rule):

$$\Phi_i = x\Phi_i^A + (1-x)\Phi_i^B, \quad i = 1,2,3. \tag{2.8}$$

There are a total of seven variables (x, Φ_1^A, Φ_2^A, Φ_3^A, Φ_1^B, Φ_2^B, and Φ_3^B), along with four independent restraints [$\Phi_1^A + \Phi_2^A + \Phi_3^A = \Phi_1^B + \Phi_2^B + \Phi_3^B = 1$ and two ($i = 1,2$) lever rules from Eq. (2.8)]. Thus given a point (Φ_1, Φ_2, Φ_3), one has three independent adjusting parameters (e.g., the orientation angle and the length of the tie line as well as the fraction of the solution that separates into phase A). By scanning through these three parameters, one can find a minimal free energy with its corresponding two phases at $(\Phi_1^A, \Phi_2^A, \Phi_3^A)$ and $(\Phi_1^B, \Phi_2^B, \Phi_3^B)$. For a fixed temperature, the set of binodal points are connected to form curves in a ternary diagram according to the phase rule.

In addition to the above restricted condition whereby the equilibria between two coexisting phases are maintained by the equality of chemical potentials of the polyelectrolyte, salt, and solvent, it is possible for the various ions to undergo ion-exchange between the coexisting phases. Now, in establishing the emergent Donnan equilibrium, the chemical potentials of all ions (polyelectrolyte, counterions, and salt cations and anions) and solvent are equal in the coexisting phases. In deriving the phase diagram, we use a similar numerical procedure as above, but now with a four-dimensional minimization of the free energy. Since there are five distinct compositions in each phase and x is the fraction of one phase in the phase-separated system, there are eleven unknown variables. Combining the lever rule for each of the species with the incompressibility and electroneutrality criteria for each of the phases, the number of unknown variables is reduced to four. The four-dimensional minimization procedure is carried out by the downhill simplex algorithm.[40]

III. RESULTS AND DISCUSSIONS

In our calculations, the charged polyelectrolyte segments have an effective valency $Z_p = 1$, and the counterions from dissolved polyelectrolyte chains and negative salt ions are monovalent, i.e., $Z_c = Z_- = 1$. The experimentally relevant parameter temperature (T) appears through both the short-ranged hydrophobic interaction (χ parameter) and the electrostatic interaction (ℓ_B). We express the strength of the electrostatic interaction through a reduced temperature t defined as $t \equiv \ell/(4\pi\ell_B)$. The temperature dependence of the χ parameter is chosen as $\chi = \theta/(2T)$, where θ is the Flory theta temperature. We rewrite the inverse temperature dependence of χ as $\chi \equiv a/(20\pi t)$. The parameter $a(=10\pi\epsilon k_B\theta/e^2)$ reflects the magnitude of the θ temperature and is taken as a measure of the hydrophobic interaction. When $a = 1$, the aqueous system corresponds roughly to a χ value of 0.6. In the present work, we explore the range of $0 \le a \le 1$. The experimental realization of a particular value of a might be challenging in terms of the choices of solvent and polymer backbone. Our theoretical results are presented over a range of a values with the aim of identifying various global features of polyelectrolyte phase behavior. Furthermore, we have taken $w_{pp} = 0 = w_{ss}$, so that $w_{ps} = \chi$. As demonstrated in Ref. 27, the effect of degree of polymerization on the phase behavior is only weak. This is due to the fact that the counterion entropy dominates the free energy in comparison to the translational entropy of the polymer chains. In view of this, we present below results for representative values of N.

A. The salt-free case

We first examine the phase diagrams for polyelectrolyte solutions without any added salt. In the studies of salt-free

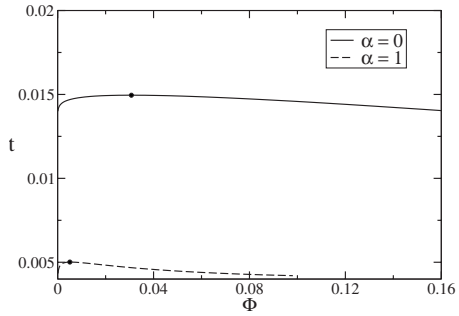

FIG. 1. Coexistence curves for a salt-free polyelectrolyte solution with degree of ionization $\alpha=0$ and 1 (the hydrophobic parameter is set to $a=1/2$). The dots at the top of the curves represent the critical points.

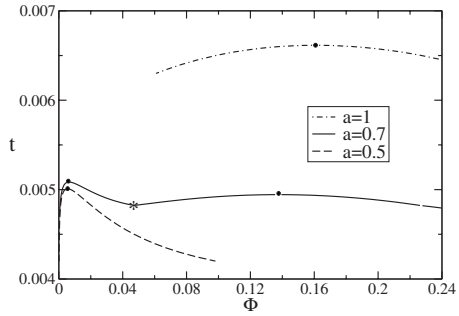

FIG. 3. Coexistence curves for a salt-free polyelectrolyte solution with various values of the hydrophobic parameter a (the degree of ionization is set to $\alpha=1$). The dots represent critical points and the asterisk represents a triple point for intermediate values of a.

polyelectrolyte solutions the chain length is set to $N=1000$. By varying parameters a and α, we follow the interplay between the chain-solvent interactions, represented by the hydrophobic parameter a, and the degree of ionization α. First we fix a to be 1/2 and the calculated phase diagrams for $\alpha=0$ and 1 are shown in Fig. 1, where the reduced temperature t is plotted against the polymer concentration Φ. We find that the critical temperature and thus the onset of phase separation for charged polymers ($\alpha=1$) are much lower than those for uncharged polymer solutions ($\alpha=0$). Therefore, by endowing charges to the polymer chains, the experimental domain for the formation of the homogeneous phase is significantly enhanced. Moreover, for the case $N=1000$, the critical density of uncharged polymer solutions is much larger than that for a strong polyelectrolyte ($\alpha=1$), implying that the fully ionized polyelectrolyte solution has a highly asymmetric phase diagram. The enhanced asymmetry of the phase diagram is consistent with the RPM results.[27]

Before we consider the effect of the parameter a, it must be recognized that the size of the counterions plays a crucial role in the phase behavior. In order to demonstrate this feature, we have calculated the phase diagrams with counterion diameter ℓ and in the limit of $\ell \to 0$. Furthermore, in real systems, the size of the counterion could depend on the chemical nature of monomers and solvent, namely, the parameter a. In the present paper, the self-consistent coupling between a and ℓ is not addressed. The results presented in Fig. 2 are labeled, respectively, as DH+RPM and DHLL. We find that the critical temperature of the DHLL, which treats the small ions as point charges, is more than five times larger than the critical temperature of the DH+RPM model. Since the ions have gained effective hydrated sizes in aqueous solutions, this results in a reduced strength in electrostatic interactions and consequently lowers the critical temperature.

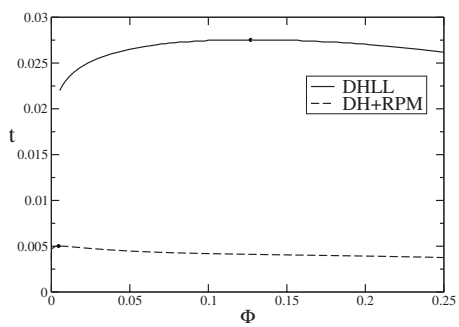

FIG. 2. Comparison of coexistence curves between the DH+RPM and the DHLL results. In the DHLL, the small ions are approximated as point charges, while in the DH+RPM model the small ions are represented by uniform hard spheres of diameter ℓ. The parameters are set as $N=1000$, $\alpha=1$, and $a=1/2$. The dots represent critical points.

The effect of the hydrophobic interaction is illustrated in Fig. 3, where we have fixed the degree of ionization α to be 1 and the parameter a is varied. When a is large the phase diagram is typical of uncharged polymer solutions, as expected. On the other hand, for small values of a, the highly asymmetric phase diagram has more resemblance to that of an electrolyte solution. Remarkably, when the hydrophobic parameter has an intermediate value (e.g., $a=0.7$), the phase diagram exhibits two critical points as well as a triple point. This implies that there are two branches of liquid-liquid phase separations, one corresponding to the hydrophobicity-induced phase separation characteristic of uncharged polymer solutions, and the other corresponding to the electrostatics-induced phase separation typical of electrolyte solutions. These two branches can be monitored as the loci of the critical points for these two liquid-liquid phase transitions. Each branch ends at a critical end point. Depending on the values of a and α, there is an intermediate polymer density at which a triple point emerges. The emergence of the triple point occurs only for a above a threshold value, which in turn depends on α. Figures 4(a) and 4(b) show the dependencies of the critical temperature and critical polymer concentration for the two branches as well as the triple points (the latter of which being represented through dotted lines) on the hydrophobicity parameter a and the degree of ionization α. We find that at low degree of ionization there is only one liquid-liquid phase separation phenomenon where the two branches have merged into one dominated by the hydrophobicity effect. On the other hand, for α values above a threshold value, the distinction between the two critical branches emerges, as is evident in Figs. 4(a) and 4(b). The triple points are represented by the dashed curve connecting the critical end points of the two branches.

B. Monovalent salt

In our investigation of the effect of added monovalent salt on the phase behavior of polyelectrolyte solutions, we have taken the parameters $N=100$ and $\alpha=1$ throughout our

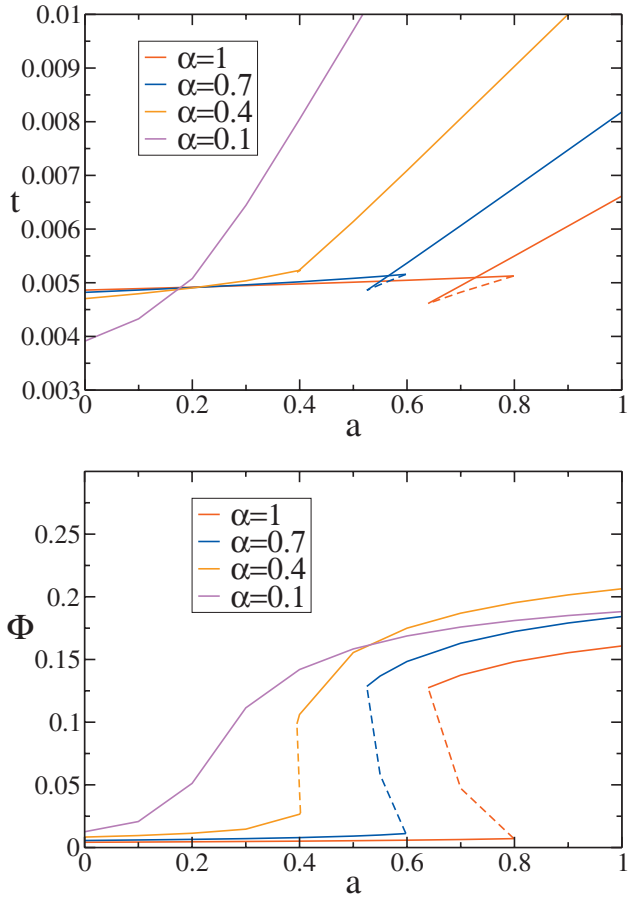

FIG. 4. (Color) (a) Critical temperature and (b) critical polymer volume fraction versus the hydrophobic parameter a for various degrees of ionization α. The dashed lines are triple points.

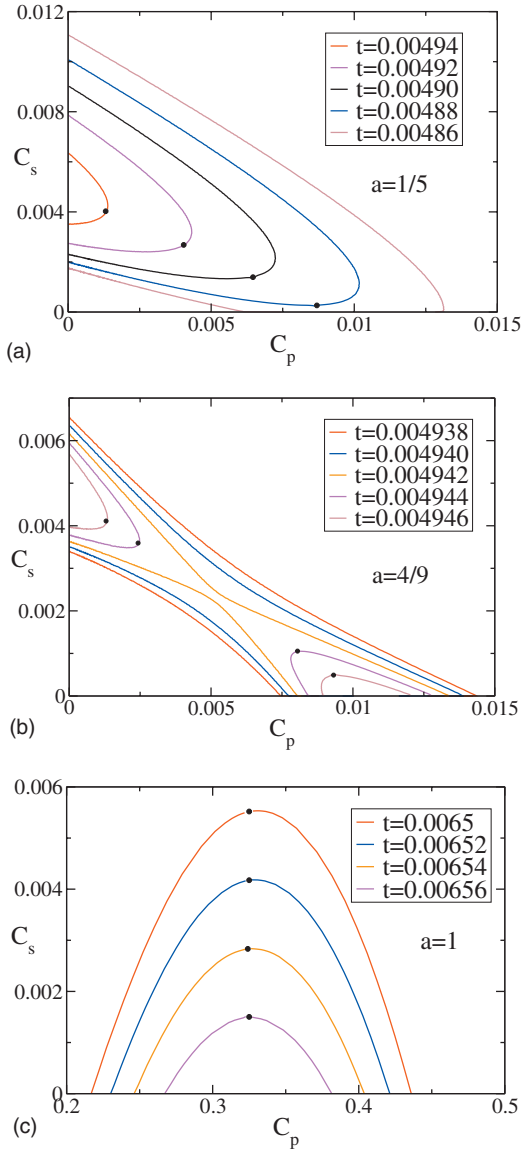

FIG. 5. (Color) Coexistence curves for polyelectrolyte solutions with added monovalent salt for (a) $a=1/5$, (b) $a=4/9$, and (c) $a=1$. The dots represent the various critical points.

calculations. For convenience we define $C_p \equiv \Phi + \Phi_c$ to be the volume fraction consisting of polymers and their counterions, and $C_s \equiv \Phi_+ + \Phi_-$ to be the salt volume fraction. In the case of monovalent salt we assume for simplicity that the monovalent salt cations and polyelectrolyte counterions are distinct ionic species. In the presence of monovalent salt ($Z_+=1$) the phase behavior yields rich features for various values of the hydrophobic parameter a, as illustrated in Figs. 5(a)–5(c), where C_s is plotted against C_p. For example, in Fig. 5(a), we find that for a relatively lower a (in this example $a=1/5$) value, the phase demixing region grows out from the left side of the plot and leans toward the bottom right area. For each temperature, the binodal consists of two branches which are linked by tie lines, while a critical point exists at the point where the two branches meet. As for a relatively larger hydrophobic parameter a, the binodals move up from the bottom (lower C_s) and the region of homogeneity is reduced [as shown in Fig. 5(c)] as the temperature is reduced. For an intermediate a value, such as $a=4/9$, we observe two sets of binodal curves at a fixed temperature (say, $t=0.004\,946$ or $0.004\,944$), each with its own critical point, as is shown in Fig. 5(b). As the temperature is lowered, the two demixing regions become broader and eventually meet with each other and merge into one demixing region at a temperature of $t \approx 0.004\,943$.

As in the salt-free case, we observe the existence of triple points under pertinent conditions. For example, in Fig. 6 we show that for $t=0.0048$ and $a=0.7$ (while $\alpha=1$ and $N=1000$) the phase diagram shows a triple point and a three-phase coexisting region.

C. Multivalent salt

We have computed the coexistence curves for polyelectrolyte solutions with added multivalent salts, where the cation is taken to be either divalent or trivalent. As described in Sec. II, we ignore all consequences of the bridging effect arising from the multivalency of the cation. The following results are obtained for the parameter setting: $N=100$, $\alpha=1$, and $a=1/2$. For the divalent and trivalent salt cases ($Z_+=2$ and 3) we show in Figs. 7(a) and 7(b) that the coexistence curves exhibit trends that are qualitatively different from those for monovalent salt. Here we observe that the demixing behavior occurs at higher temperatures, at which the pure polyelectrolyte solution does not phase separate unless some

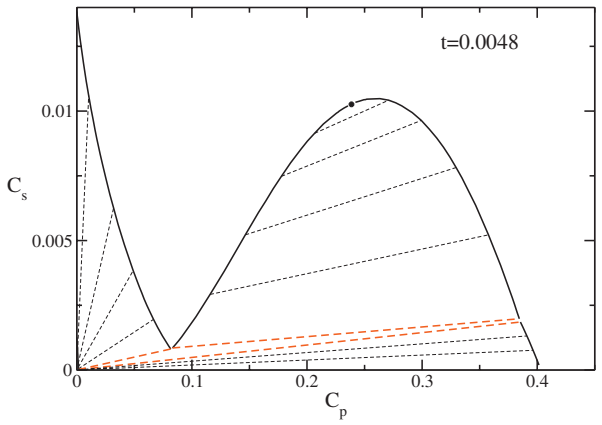

FIG. 6. (Color) Phase diagrams of polyelectrolyte solutions with the addition of monovalent salt for $a=0.7$. The dashed lines are tie lines. Note that there is a three-phase coexisting region inside the dashed red triangle.

multivalent salt is added into the solution. Again for each fixed temperature, the binodal has two branches connected through tie lines. By using the log-log plot one can find a good qualitative agreement between the phase diagrams shown in Figs. 7(a) and 7(b), and many experimental observations on flexible polyelectrolyte solutions and DNA solutions with added multivalent salt.[1,2,4] The experimental data have been marked in literature as precipitation curves, whereas our theoretical calculations show that this phenomenon is indeed liquid-liquid phase separation. In particular, if one fixes the polymer concentration in the solution and increases the multivalent salt concentration, one often finds the precipitation and reentrant phenomenon. It is to be noted that the slope of the upper branch in our calculated coexistence curves is negative, whereas the slope is often positive in the experimental observations at room temperature. However, as

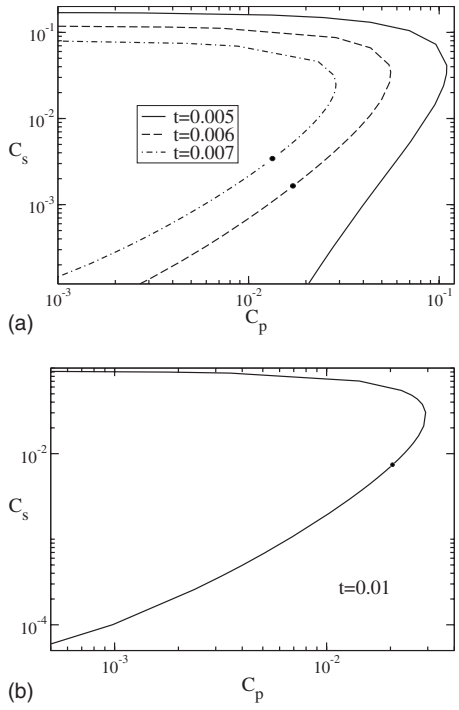

FIG. 7. Liquid-liquid coexistence curves for polyelectrolyte solutions with added (a) divalent and (b) trivalent salts ($\alpha=1$, $N=100$, and $a=1/2$).

discussed in Sec. III D, the method we used to derive phase diagrams in this subsection is based on an additional constraint. Accounting of the ion exchange between the coexisting phases changes the slope of the upper branch to positive while maintaining all other qualitative features of the liquid-liquid phase separation intact.

D. Ion exchange

We now proceed to address the ion exchange effect between the coexisting phases. In Sec. III C, we treated the solution as a ternary mixture, while the thermodynamic equilibrium is achieved via equilibrating the chemical potential of the components (polymer, salt, and solvent) in each phase. However, with this treatment, we have set proportional relations as the following:

$$Z_p\alpha\Phi = Z_c\Phi_c \quad \text{and} \quad Z_+\Phi_+ = Z_-\Phi_-. \tag{3.1}$$

Equation (3.1) does hold when the solution is homogeneous. However, this proportionality relation might not be held in general when phase separation occurs. Instead one should use

$$Z_p\alpha\Phi^0 = Z_c\Phi_c^0 \quad \text{and} \quad Z_+\Phi_+^0 = Z_-\Phi_-^0 \tag{3.2}$$

and

$$Z_p\alpha\Phi^A + Z_-\Phi_-^A = Z_c\Phi_c^A + Z_+\Phi_+^A,$$

$$Z_p\alpha\Phi^B + Z_-\Phi_-^B = Z_c\Phi_c^B + Z_+\Phi_+^B. \tag{3.3}$$

According to Eq. (3.2), the initial volume fractions in the homogeneous phase naturally obey the proportionality relation. However when phase separation occurs, the ions may exchange from one phase to another, as in each phase the restricted proportionality relation is replaced by the overall charge neutrality [Eq. (3.3)]. The ion exchange effect is expected to be prominent if the solution contains multivalent salt. This is because when phase separation emerges, the multivalent cations tend to get into the phase with larger polymer density. In this regard the monovalent counterions will be released and therefore the system entropy will be increased. The mechanism is similar to the counterion adsorption. In an effort to assess the magnitude of only the ion exchange effect, we do not consider in the present calculations the structural effects arising from ion bridges due to the binding of counterions to multiple polymer segments. Although such local effects are ignored in the present theory, the correct Donnan criteria are explicitly taken into account in arriving at the thermodynamics of multicomponent polyelectrolyte solutions.

When the ion exchange effect is considered, we are allowing an extra degree of freedom in the free energy minimization as already mentioned in Sec. II. The spinodals and binodals in the phase diagrams are now surfaces, instead of curves. In Figs. 8(a) and 8(b) the phase diagram with the addition of trivalent salt at $t=0.02$ is shown via two different representations. First, to present our results in a simple manner, we use a two-dimensional representation of the phase diagram in Fig. 8(a). Each blue dot represents an initial set of polymer and salt volume fractions that results in phase sepa-

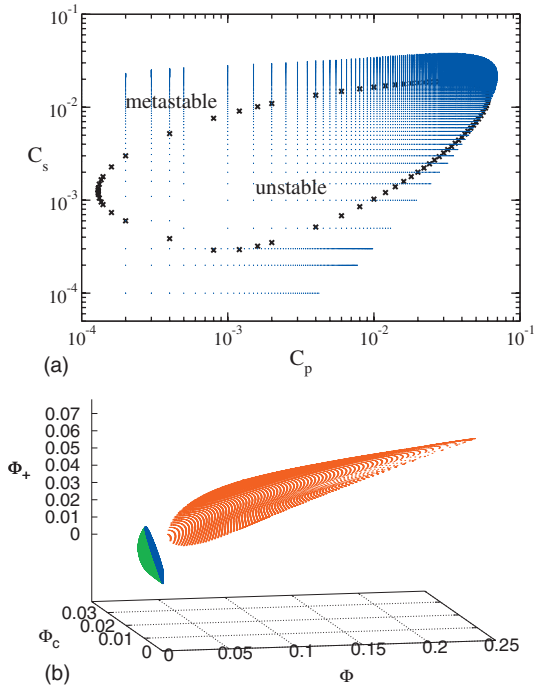

FIG. 8. (Color) Phase diagrams of polyelectrolyte solutions with added trivalent salt at $t=0.02$ by accounting for ion exchange. (a) The blue dots are the initial polymer and salt volume fractions that result in phase separation. The crosses constitute the boundary for spinodal decomposition. (b) The binodal surfaces show the coexistence of two phases represented by the green and red dots. The blue area represents the set of initial volume fractions that result in phase separation [the same data of (a) shown in the three dimensional phase space]. The parameter setting is $N=100$, $\alpha=1$ and $a=1/2$.

ration. Here we observe a similar behavior compared to our observation in Fig. 7(b) as well as the experimental results. However a detailed examination shows that the phase separation can exist even at much higher temperatures. Moreover the major difference between Figs. 7(b) and 8(a) lies in the fact that in Fig. 8(a) the system has an extra degree of freedom for ion exchange between demixed phases. In Fig. 8(b) the binodal is shown as two curved surfaces (in green and red), while the blue plane represents the full set of blue dots in Fig. 8(a). Thus for each initial set of ionic volume fractions located on the blue plane, the solution will eventually

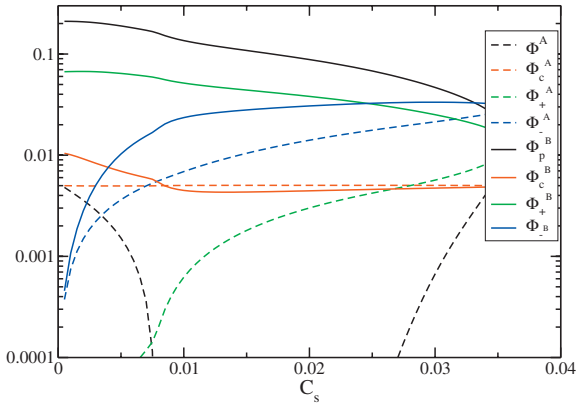

FIG. 9. (Color) The volume fractions of all charged species during the phase separation. $C_p=0.01$, while other parameter settings are the same as in Fig. 8.

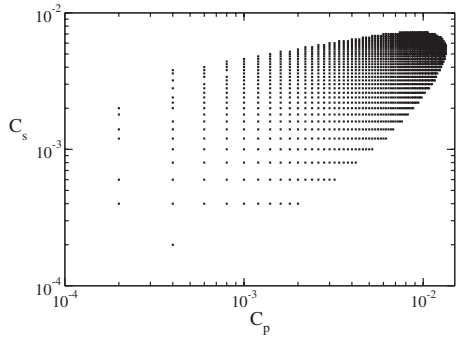

FIG. 10. Liquid-liquid phase separation with added trivalent salt at $t=0.03$. There is no unstable region (spinodal decomposition) at this temperature.

evolve into the coexistence of two phases, represented by a green dot and a red one. Note that in this temperature regime a phase separation cannot be observed for either a pure polyelectrolyte solution or a pure trivalent salt solution. Nevertheless, phase separation can occur for a polyelectrolyte solution upon the addition of very small amount of salt.

If we fix the initial volume fraction C_p and increase the initial salt volume fraction C_s, the liquid-liquid coexistence ("precipitation re-entrant") behavior can be observed. To find out the details of ionic exchange and recombination, we plot the volume fraction of all charged species in Fig. 9. By focusing on the volume fractions of polymers and trivalent cations, we observe that when the phase separation emerges, an approximate relation $(Z_p\alpha\Phi)/(Z_+\Phi_+)\approx 1$ can be obtained in the polymer-rich ("precipitated") phase B. Therefore the polymer chains and trivalent cations seem to neutralize each other in this phase. Furthermore, as C_s increases, this ratio becomes smaller than 1, which implies that in the polymer-rich phase there are now too many cations to neutralize the polymers. The two features mentioned above bear resemblances to the counterion adsorption and the overcharging mechanisms.

In our theory we can also derive the spinodal using the following condition

$$\det\left|\frac{\partial^2 f}{\partial\Phi_i\,\partial\Phi_j}\right|, \tag{3.4}$$

while the determinant is performed over a 3×3 matrix regarding three independent volume fractions such as Φ, Φ_c, and Φ_+. If an initial set of volume fractions lies inside the spinodal, then the system is thermodynamically unstable. In Fig. 8(a) such spinodal boundary [the slice of spinodal surface over the plane obeying Eq. (3.2)] is shown by crosses. However, as the temperature increases, both the spinodal and binodal surfaces become smaller and there can be possibilities that only the binodal surface intersects the plane of initial volume-fraction settings Eq. (3.2). Such example is shown in Fig. 10. Therefore, in polyelectrolyte solutions with the addition of multivalent salt, one may encounter a phase diagram that shows no spinodal decomposition.

IV. CONCLUSION

By implementing our recent theory for flexible polyelectrolyte solutions we have found several interesting results on

their phase behavior. For a pure polyelectrolyte solution without any added salt, its dual nature as an electrolyte and polymer solution is observed, as both types of liquid-liquid phase separation are shown in the phase diagrams. Under appropriate conditions, triple points and three-phase coexistence regions emerge. In the presence of monovalent salt, the phase behavior yields rich features due to the interplay of the hydrophobic interactions and the electrostatic interactions. The predicted low reduced temperature t required for the observation of phase separation indicates that this phase behavior requires large electrostatic interactions. Experimentally this can be possibly achieved through the modification of the dielectric constant of the solution.

In the presence of salt with multivalent cations, our calculated phase diagrams are seemingly similar to the precipitation–re-entrant diagrams, which are found in many experiments. However, in our theory, the "precipitation" and "re-entrant" features are actually liquid-liquid phase separations. While most qualitative features can be already seen on the phase diagrams that are calculated using a ternary mixture treatment, the correct phase behavior and a strong enhancement is shown after Donnan equilibrium is considered. The latter study exhibits the correct slopes on the phase diagrams, and it also shows strong ion exchange between the two coexisting phases.

Although a rich phase behavior results from our calculations, it is based on the M theory with only mean field arguments (as in the limiting cases of the FH and RPM theories). Nevertheless, given the success of the FH theory in describing many phenomena related to phase behavior of uncharged polymers sufficiently away from critical points, the M theory might have similar utility for solutions of flexible polyelectroltyes. As some experiments clearly demonstrate the Ising criticality for polyelectrolyte solutions, a theoretical formulation of mean-field-to-Ising crossover is needed for charged systems. Moreover, the importance of counteradsorption on charged polymer backbones as well as the ion-bridging mechanism should be elucidated to get a full understanding about the thermodynamics of polyelectrolyte solutions.

There are a few directions where the present theory can be immediately expanded. The phase behavior of charged polymers with hydrophilic backbone and nonmetallic multivalent counterions is an example. The computations presented here and in the M theory are restricted to only fully flexible polyelectrolytes without any consideration of orientational correlations between segments along the chain backbone. Further extension is in progress to address the phase behavior of semiflexible polyelectrolytes, with both backbone stiffness and electrostatic stiffness, and the onset of liquid-crystalline order.

ACKNOWLEDGMENTS

It is a pleasure to thank Mr. Bernhard Fischer for his contributions during the initial stage of this project. Acknowledgment is made to the National Science Foundation Grant No. DMR-0605833, and the Materials Research Science and Engineering Center at the University of the Massachusetts, Amherst.

[1] I. Sabbagh and M. Delsanti, Eur. Phys. J. E **1**, 75 (2000).
[2] M. Delsanti, J. P. Dalbiez, O. Spalla, L. Belloni, and M. Drifford, ACS Symp. Ser. **548**, 381 (1994).
[3] J. Pelta, F. Livolant, and J.-L. Sikorav, J. Biol. Chem. **271**, 5656 (1996).
[4] E. Raspaud, M. O. de la Cruz, J.-L. Sikorav, and F. Livolant, Biophys. J. **74**, 381 (1998).
[5] M. Saminathan, T. Anthony, A. Shirahata, L. Sigal, T. Thomas, and T. J. Thomas, Biochemistry **38**, 3821 (1999).
[6] Q. Wen and J. X. Tang, J. Chem. Phys. **121**, 12666 (2004).
[7] K. A. Narh and A. Keller, J. Polym. Sci., Part B: Polym. Phys. **31**, 231 (1993).
[8] K. A. Narh and A. Keller, J. Polym. Sci., Part B: Polym. Phys. **32**, 1697 (1994).
[9] V. M. Prabhu, M. Muthukumar, G. D. Wignall, and Y. B. Melnichenko, Polymer **42**, 8935 (2001).
[10] V. M. Prabhu, M. Muthukumar, G. D. Wignall, and Y. B. Melnichenko, J. Chem. Phys. **119**, 4085 (2003).
[11] S. Kanai and M. Muthukumar, J. Chem. Phys. **127**, 244908 (2007).
[12] F. Oosawa, *Polyelectrolytes* (Dekker, New York, 1971).
[13] T. T. Nguyen, I. Rouzina, and B. I. Shklovskii, J. Chem. Phys. **112**, 2562 (2000).
[14] K. A. Mahdi and M. Olvera de la Cruz, Macromolecules **33**, 7649 (2000).
[15] A. V. Ermoshkin and M. Olvera de la Cruz, Macromolecules **36**, 7824 (2003).
[16] M. O. de la Cruz, L. Belloni, M. Delsanti, J. P. Dalbiez, O. Spalla, and M. Drifford, J. Chem. Phys. **103**, 5781 (1995).
[17] F. J. Solis and M. Olvera de la Cruz, J. Chem. Phys. **112**, 2030 (2000).
[18] F. J. Solis and M. Olvera de la Cruz, Eur. Phys. J. E **4**, 143 (2001).
[19] J. Wittmer, A. Johner, and J. F. Joanny, Journal de Physique **5**, 635 (1995).
[20] P. B. Warren, Journal de Physique **7**, 343 (1997).
[21] K. Bergfeldt and L. Piculell, J. Phys. Chem. **100**, 5935 (1996).
[22] M. Gottschalk, P. Linse, and L. Piculell, Macromolecules **31**, 8407 (1998).
[23] D. Y. C. Chan, P. Linse, and S. N. Petris, Langmuir **17**, 4202 (2001).
[24] A. R. Khokhlov and I. A. Nyrkova, Macromolecules **25**, 1493 (1992).
[25] E. Yu. Kramarenko, I. Ya. Erukhimovich, and A. R. Khokhlov, Macromol. Theory Simul. **11**, 462 (2002).
[26] M. Muthukumar, J. Chem. Phys. **105**, 5183 (1996).
[27] M. Muthukumar, Macromolecules **35**, 9142 (2002).
[28] B. K. Fischer, MS thesis, University of Massachusetts, 2005.
[29] P. J. Flory, *Principles of Polymer Chemistry* (Cornell University Press, Ithaca, NY, 1953).
[30] D. A. McQuarrie, *Statistical Mechanics* (Harper and Row, New York, 1976).
[31] G. Stell, K. C. Wu, and B. Larsen, Phys. Rev. Lett. **37**, 1369 (1976).
[32] G. Stell, Phys. Rev. A **45**, 7628 (1992).
[33] M. E. Fisher and Y. Levin, Phys. Rev. Lett. **71**, 3826 (1993).
[34] M. E. Fisher, J. Stat. Phys. **75**, 1 (1994).
[35] S. Liu and M. Muthukumar, J. Chem. Phys. **119**, 1813 (2003).
[36] M. Beer and M. Schmidt, Macromolecules **30**, 8375 (1997).
[37] M. Muthukumar, J. Chem. Phys. **120**, 9343 (2004).
[38] A. Kundagrami and M. Muthukumar, J. Chem. Phys. **128**, 244901 (2008).
[39] R. Horst, Macromol. Theory Simul. **4**, 449 (1995).
[40] W. H. Press, S. A. Tuokolsky, W. T. Wetterling, and B. P. Flannery, *Numerical Recipes: The Art of Scientific Computing*, 3rd ed. (Cambridge University Press, New York, 2007).